

THE LONG-RANGE CYTOTOXIC EFFECT IN TUMOR-BEARING ANIMALS

*B.I. Gerashchenko**, *N.M. Ryabchenko*, *O.A. Glavin*, *V.M. Mikhailenko*

R.E. Kavetsky Institute of Experimental Pathology, Oncology and Radiobiology, National Academy of Sciences of Ukraine, Kyiv 03022, Ukraine

Aim: The relationship between cancer and patient health is still of great interest for experimental and clinical oncology. The tumor can adversely affect surrounding and distant tissues as well. However, effects of the tumor on distant tissues are much less studied than its effects on surrounding tissues. This study was aimed to test whether the tumor could trigger cytotoxic and/or genotoxic signals with respect to the distant proliferative tissue such as bone marrow. **Materials and Methods:** Rats were subcutaneously implanted with Guerin carcinoma cells, and on the 12th and 18th days after implantation both cytotoxic and genotoxic effects were assessed by flow cytometry in acridine orange stained unfractionated bone marrow cells isolated from femur. The cytotoxic effect was assessed using ratios of the following cell populations: total nucleated cells (TNC)/total enucleated erythrocytes (TE); polychromatic erythrocytes (PCE)/normochromatic erythrocytes (NCE). The genotoxic effect was assessed by quantification of micronucleated PCE (MNPCE) within the population of PCE. **Results:** A significant cytotoxic effect was observed in tumor-bearing animals on the 12th and 18th days after implantation (\approx 2-fold decrease in both TNC/TE and PCE/NCE ratios compared with corresponding parameters in control animals). There was also a genotoxic effect in these animals (a slight increase in the number of MNPCE), however, this effect was insignificant. The PCE/NCE ratio reversely correlated with the tumor weight which is suggestive of the link between erythropoietic cytotoxicity and tumor progression. **Conclusion:** Cytotoxic insult to the bone marrow is likely to be associated with the mechanism(s) triggered by distantly located tumors whose growth may correlate with the cytotoxic effect.

Key Words: Guerin carcinoma, bone marrow, cytotoxicity, TNC/TE ratio, PCE/NCE ratio, flow cytometry.

The tumor-host interaction is a complex process that puzzles experimental and clinical oncologists for decades. The problem of interaction of the tumor with the host was well summarized by Kavetsky in 1977 [1]. Even though at present time new and more accurate techniques are being used in cancer research, much work is yet to be done to wider uncover this problem. It is not surprising that a large body of work has been focused on the study of effects of a tumor on surrounding (adjacent) tissues and *vice versa*, a model which is attractive for several reasons: it is convenient in terms of experimental design planning, and it is informative and precise in terms of visualization of effects and dissection of mechanisms. Tumor cells by interacting with its stroma have been found to change their phenotype and biological properties [2, 3]. On the other hand, tumors have been shown to affect surrounding noncancerous cells causing DNA damage [4–6]. As for adverse effects of tumors on distant tissues, there is the only known fact that they can induce a complex DNA damage (double strand breaks (DSBs) and oxidatively induced clustered DNA lesions (OCDLs)), particularly in proliferative tissues

(skin and crypts in the gastrointestinal organs) [7]. Since a proliferative tissue contains a large fraction of S-phase cells sensitive to DNA DSB formation (as evidenced by phosphorylation of histone H2AX [8, 9]), proliferation of cells in this tissue exposed to DNA damaging agents could be delayed due to DNA repair processes. Cytotoxic/genotoxic insults frequently impair the proliferating and maturational abilities of cells.

To test whether such a highly proliferative hematopoietic tissue as bone marrow is among sensitive targets for distantly located tumors, adult male rats were subcutaneously implanted with Guerin carcinoma (GC; uterine adenocarcinoma of rats) cells, and then on the 12th and 18th days after implantation cytotoxic and genotoxic effects were assessed in hematopoietic cells of unfractionated bone marrow according to the techniques proposed by Criswell *et al.* [10, 11]. In brief, the cytotoxic effect was assessed by flow cytometry using two parameters: 1) ratio of the population of total nucleated cells (TNC) to the population of total enucleated erythrocytes (TE) composed of immature polychromatic (PCE) and mature normochromatic erythrocytes (NCE); 2) ratio of the population of PCE to the population of NCE [10]. The TNC/TE ratio is used to determine overall myelosuppression, while the PCE/NCE ratio is used to specifically determine suppression of erythropoiesis. Clastogenic agents that target the process of DNA replication are known to suppress cell proliferation thus causing decreases of these ratios [10, 12, 13]. TNC/TE and PCE/NCE ratios are key components of cytotoxicity assessment, among which the PCE/NCE ratio is most frequently used with the micronucleus (MN) test. The genotoxic effect was assessed by flow cytometric counting of micronucleated PCE (MNPCE) within the population of PCE [11].

Received: October 25, 2011.

*Correspondence: Fax: (380 44) 258 1656

E-mail: biger63@yahoo.com

Abbreviations used: AO – acridine orange; CCL2 – chemokine (C-C motif) ligand 2; DSB – double strand break; EDTA – ethylenediaminetetraacetic acid; FBS – fetal bovine serum; GC – Guerin carcinoma; MNPCE – micronucleated polychromatic erythrocytes; NCE – normochromatic erythrocytes; OCDL – oxidatively induced clustered DNA lesion; PBS – phosphate buffered saline; PCE – polychromatic erythrocytes; ROS – reactive oxygen species; SDS – sodium dodecyl sulfate; TE – total enucleated erythrocytes; TNC – total nucleated cells.

MATERIALS AND METHODS

Animal tumor model. Adult random-bred male rats (250–300 g) were obtained from the vivarium of R.E. Kavetsky Institute of Experimental Pathology, Oncology and Radiobiology, NAS of Ukraine (Kyiv, Ukraine). Guerin carcinoma (GC, or T8) cells were obtained from the Bank of Cell Lines from Human and Animal Tissues of the aforementioned Institute. Up to 90% of rats can be successfully implanted with this type of cells regardless of the strain of animals used for implantation [14]. The work with animals was performed according to the rules of local Ethic Committee. Tumors were implanted by subcutaneous injection (dorsally into the left flank) of 2.2×10^6 GC cells suspended in 0.5 ml of sterile physiological solution. On the 12th and 18th days after implantation animals were sacrificed. Tumors attached to the inner side of the skin were carefully removed with scissors and then weighed. Although this animal tumor model may be not highly syngeneic, this is not likely to be an issue, since the goal of our work was not investigation of a specific mechanism of the tumor-host interaction or anti-cancer drug delivery.

Bone marrow isolation. Femur removal and bone marrow isolation procedures were performed as proposed [10]. Bone marrow cells were thoroughly flushed from the femur with 3 ml of FBS and kept at +4–6 °C before use.

Specimen processing and fixation. Bone marrow samples were kept in a fridge no longer than 1.5 h before they were resuspended by vortexing and centrifuged at $300 \times g$ for 5 min. In general, specimen processing and fixation procedures were performed as proposed [10]. The supernatant was discarded followed by washing cells in 5 ml of PBS. After centrifugation them at $300 \times g$ for 5 min, the supernatant was discarded and then the pellet was resuspended in 2 ml of PBS by vortexing. Cell aggregates were dissociated by gentle syringing of the suspension through a 21-gauge needle. While vigorous vortexing, 0.2 ml of processed whole bone marrow was added to 5 ml of fixative solution: 1% glutaraldehyde (v/v) in PBS with 30 μ g/ml of SDS (Merck, Germany). In this solution, erythrocytes become spherical [15]. Cells were fixed for 5 min and then centrifuged for an additional 5 min at $300 \times g$. The supernatant was removed followed by resuspension of cells in 0.5 ml of PBS.

Fluorescence staining. This procedure was performed in accordance with the published protocol [11]. Solution A was prepared by dissolving in 100 ml (final volume) of distilled H₂O of the following components: 0.1 ml Triton X-100 (Loba Chemie, Austria), 8 ml 1.0 N HCl, and 0.877 g NaCl. Solution B was prepared by mixing of 37 ml 0.1 M anhydrous citric acid with 63 ml 0.2 M Na₂HPO₄ (pH 6.0) and adding 0.877 g NaCl, 34 mg EDTA disodium salt (Sigma, USA) and 0.6 ml of acridine orange (AO; Sigma) stock solution (1 mg/ml). Fixed cells (0.2 ml of cell suspension) were mixed with ice-cold Solutions A and B (0.4 and 1.2 ml, respectively) in a 12 \times 75 mm centrifuge tubes. While shaking, cells were stained on ice for 30 min in the dark.

They were then centrifuged at $300 \times g$ for 5 min. After the supernatant was carefully removed, 1 ml of PBS was added to resuspend the pellet. Before flow cytometry, the cell suspension was gently syringed through a 21-gauge needle to mainly analyze single cells.

Flow cytometry. Samples were analyzed on an EPICS XL flow cytometer (Beckman Coulter, USA) equipped with a 15 mW argon-ion laser (488 nm). Instrument settings were in general the same as recommended [10, 11]. The forward light scatter (related to cell size) and the side light scatter (related to intracellular granularity) signals were collected in linear mode. The fluorescence of DNA- and RNA-bound AO was measured in the green fluorescence channel (FL1) through a 525/10-nm band-pass filter with logarithmic amplification and in the far red fluorescence channel (FL4) through a 675/10-nm band-pass filter with logarithmic amplification, respectively. An acquisition rate was ≈ 1000 cells per second. At least 1.5×10^5 events were collected for each sample. Analysis of the data was performed with the publicly available software “WinMDI” developed by Dr. J. Trotter (<http://facs.scripps.edu/software.html>). Cells were gated on forward scatter versus side scatter histograms to eliminate debris and aggregates from analysis, although microscopical observation showed that their numbers were very low. On the Forward scatter versus FL1-Height histogram, events that represent populations of TNC, PCE, and NCE were compartmentalized well enough to perform analysis (Fig. 1). Although Criswell *et al.* [10] proposed to use the FL4- versus FL1-Height histogram for quantification of TNC, PCE, and NCE, the Forward scatter versus FL1-Height histogram (presented in Fig. 1) can also be used for this purpose (both histograms gave similar apportionments of these cells). For cytotoxicity assessment, TNC/TE (where TE = PCE + NCE) and PCE/NCE ratios were used [10]. For genotoxicity assessment, MNPCE (shown by the arrow; Fig. 1) were defined within the population of PCE (shown in the region R2; Fig. 1), and then their number was calculated per 1000 PCE [11]. Since levels of micronucleated NCE usually correlate with levels of MNPCE, they were not analyzed.

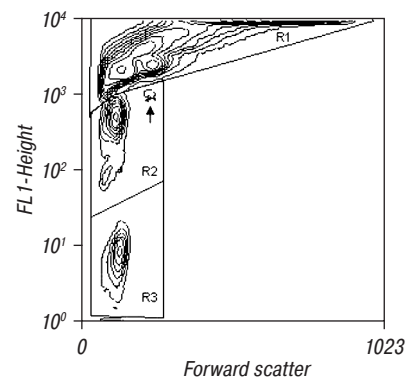


Fig. 1. Forward scatter versus FL1-Height contour plot of AO-stained unfractionated bone marrow cells that were isolated from the femur of control (intact) rat. The apportionment of TNC (in the region R1), PCE (in the region R2), and NCE (in the region R3) is 83.1, 10.8, and 6.1%, respectively. Therefore, ratios PCE/NCE and TNC/TE (where TE = PCE + NCE) are 1.8 and 4.9, respectively. The arrow shows the location of MNPCE whose frequency is 4.5/1000 PCE

Statistical analysis. The statistical significance of differences between mean values was assessed by the Student's *t*-test. Values $P < 0.05$ were considered as statistically significant.

RESULTS

In the bone marrow isolated from femurs of GC-bearing rats on the 12th and 18th days post-implantation there was about a 2-fold drop in both TNC/TE and PCE/NCE ratios compared to corresponding controls ($P < 0.05$; Fig. 2). These ratios were not sufficiently changed with the time post-implantation ($P > 0.05$; Fig. 2). Levels of MNPCE in the bone marrow of GC-bearing rats on the 12th and 18th days post-implantation were slightly higher than the level of MNPCE in the bone marrow of the control group of animals (increasing trend), although these elevations were insignificant ($P > 0.05$; Fig. 3).

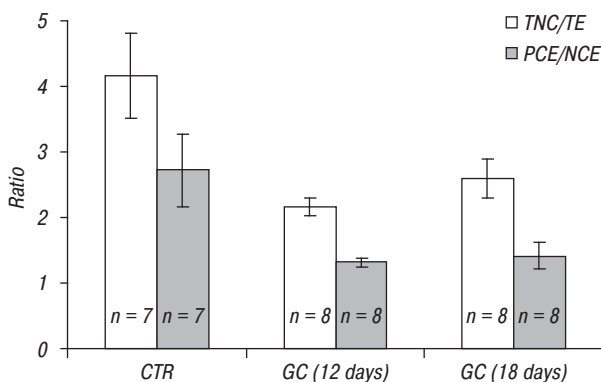


Fig. 2. TNC/TE and PCE/NCE ratios obtained from flow cytometric analysis of AO-stained bone marrow cells that were isolated from femurs of control rats (denoted as CTR) and GC-bearing rats on the 12th and 18th days post-implantation (denoted as GC (12 days) and GC (18 days), respectively). Data shown are the mean \pm standard error of the mean

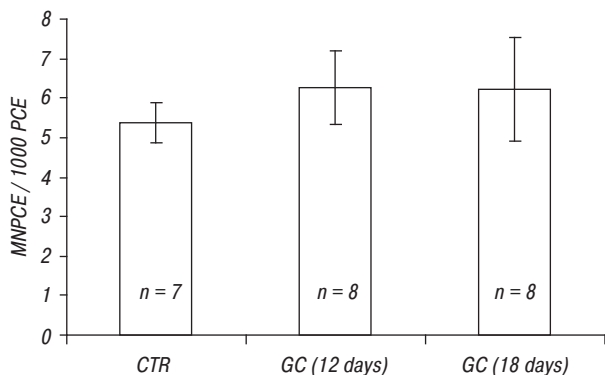


Fig. 3. Frequencies of MNPCE obtained from flow cytometric analysis of AO-stained bone marrow cells that were isolated from femurs of control rats (denoted as CTR) and GC-bearing rats on the 12th and 18th days post-implantation (denoted as GC (12 days) and GC (18 days), respectively). Data shown are the mean \pm standard error of the mean

To assess whether the cytotoxic effect depends upon the tumor progression, we generated the scatter plot of tumor masses and corresponding PCE/NCE ratios (Fig. 4). This plot shows that in the majority of GC-bearing animals the PCE/NCE ratio reversely correlated with the tumor mass. However, the slope of the regression line depended upon the time passed since implantation of tumor cells. For

the data collected from animals that carried tumors for up to 18 days, compared with the data collected from animals that carried tumors for up to 12 days, the slope of the regression line was markedly steeper (Fig. 4). Unlike the plot of PCE/NCE ratios versus tumor masses, the plot of TNC/TE ratios versus tumor masses showed a much sparser distribution of the data points whose regression lines were strictly horizontal, which is indicative of lack of correlation between these two parameters (data not shown). On the 12th and 18th days post-implantation the tumor mass values were 5.2 ± 0.6 and 6.4 ± 2.0 g, respectively (data shown are the mean \pm standard error of the mean).

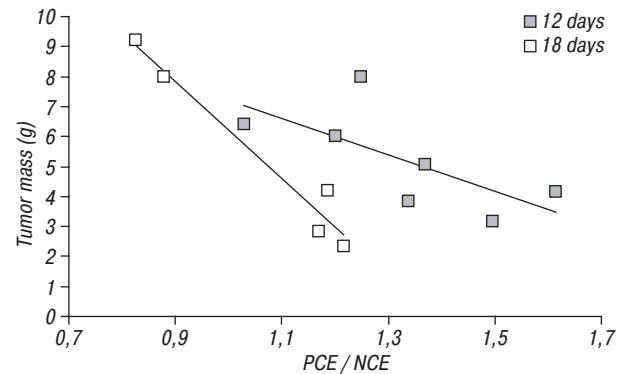


Fig. 4. Scatter plot generated from data points of tumor mass values and corresponding PCE/NCE ratio values. Distributions of data points acquired from GC-bearing rats on the 12th and 18th days post-implantation are shown by closed boxes (grey) and open boxes (white), respectively

DISCUSSION

A significant decrease in both TNC/TE and PCE/NCE ratios is indicative of serious cytotoxic insult to the bone marrow of GC-bearing rats. This insult is likely to affect a large number of cells residing in the bone marrow as evidenced by ≈ 2 -fold decrease in the TNC/TE ratio (Fig. 2). Cytotoxic effects in tissues distant to sites of implanted tumors have not been previously reported. As for genotoxicity in the bone marrow of GC-bearing rats, this effect, perhaps, exists to some extent (a slight elevation in the number of MNPCE; Fig. 3). More studies with a larger cohort of animals are probably needed to fully uncover this issue. At first it might seem that cytotoxicity in the bone marrow of GC-bearing animals does not depend on tumor growth (e.g., there was no further decrease in TNC/TE or PCE/NCE ratios, and there was no further increase in the level of MNPCE, if the data collected from rats that carried tumors for up to 18 days are compared with the data collected from rats that carried tumors for up to 12 days; Fig. 2). Nevertheless, correlation analysis of tumor masses and corresponding PCE/NCE ratios did reveal tumor growth dependent cytotoxicity in the bone marrow, namely erythropoietic cytotoxicity (Fig. 4). Perhaps, erythropoietic cells are more susceptible to tumor-associated cytotoxic stress than cells of other lineages. Impaired erythropoiesis is known to frequently accompany cancer-related anemia [16]. Inflammatory cytokines, whose production is induced by cancer, suppress erythroid progenitor

cell proliferation and erythropoietin production as well [17]. Thus, the PCE/NCE ratio appears to be a valuable parameter to monitor progression/regression of tumors that are capable of affecting erythropoiesis.

Since cytotoxicity is often accompanied by DNA lesions, we cannot exclude the possibility of DNA damage in the bone marrow of rats implanted with GC. If a complex DNA damage occurs, its repair can be delayed thus causing suppressed cell proliferation, which is one of the cytotoxicity manifestations. An insignificant genotoxic effect observed in this study (a slight elevation in the number of MNPCE; Fig. 3), perhaps, supports an assumption that DNA damage may occur in the bone marrow of rats implanted with GC. Redon *et al.* [7] in their recent study on mice that were subcutaneously implanted with tumors, such as B16 melanoma, M5076 sarcoma, and COLON26 carcinoma, have reported the induction of complex DNA damage (DSBs and OCDLs) in distant proliferative tissues, particularly in skin and crypts of gastrointestinal organs. Similar DNA lesions could be in our study. However, the most intriguing issue in this “tumor-induced bystander effect” is mechanism of its induction. Tumor-associated macrophages, major players of cancer-related inflammation [18], have been found in aforementioned mouse tumors, and also, increased amounts of activated macrophages have been found in gastrointestinal tissues and skin [7]. Moreover, cytokine CCL2 (also known as monocyte chemoattractant protein-1), which is linked to chronic inflammation conditions and cancer [19], has been shown as an essential mediator in tumor-induced DNA damage in distant tissues [7]. This cytokine has been reported to be secreted by tumor cells, normal tissues, and immune cells [20]. However, in the study by Redon *et al.* [7], CCL2 is unlikely to be produced by the tumor cells themselves, since tumor-bearing CCL2-deficient mice, compared with tumor-bearing CCL2-proficient mice, showed neither the presence of this cytokine in the serum nor elevation of DNA damage (DSBs or OCDLs) in distant tissues [7]. To induce DNA damage in a distant tissue, tumor cells have to activate resident or distant immune cells that after being activated release genotoxic substances including ROS. Tumor cells are likely to activate immune cells via direct and indirect contacts as well [7], since tumor cells are capable of secreting a variety of cytokines and other factors [21].

The fact that a tumor together with expressed CCL2 is an inevitable prerequisite to induce in distant tissues DNA lesions (whose level correlates with proliferative state of the tissue) may also take place in our study. Tumor growth dependent erythropoietic cytotoxicity in GC-bearing rats is likely to be a part of the common mechanism of tumor-induced inflammatory response.

REFERENCES

1. Kavetsky RE. The interaction of the organism and the tumor. Kiev: Naukova Dumka, 1977. 235 p. (In Russian).
2. Liotta LA, Kohn EC. The microenvironment of the tumor-host interface. *Nature* 2001; **411**: 375–9.
3. Zigrino P, Löffek S, Mauch C. Tumor-stroma interactions: their role in the control of tumor cell invasion. *Biochimie* 2005; **87**: 321–8.
4. Hussain SP, Hofseth LJ, Harris CC. Radical causes of cancer. *Nat Rev Cancer* 2003; **3**: 276–85.
5. Jüngst C, Cheng B, Gehrke R, *et al.* Oxidative damage is increased in human liver tissue adjacent to hepatocellular carcinoma. *Hepatology* 2004; **39**: 1663–72.
6. Nowsheen S, Wukovich RL, Aziz K, *et al.* Accumulation of oxidatively induced clustered DNA lesions in human tumor tissues. *Mutat Res* 2009; **674**: 131–6.
7. Redon CE, Dickey JS, Nakamura AJ, *et al.* Tumors induce complex DNA damage in distant proliferative tissues *in vivo*. *Proc Natl Acad Sci USA* 2010; **107**: 17992–7.
8. Burdak-Rothkamm S, Short SC, Folkard M, *et al.* ATR-dependent radiation-induced gamma H2AX foci in bystander primary human astrocytes and glioma cells. *Oncogene* 2007; **26**: 993–1002.
9. Burdak-Rothkamm S, Rothkamm K, Prise KM. ATM acts downstream of ATR in the DNA damage response signaling of bystander cells. *Cancer Res* 2008; **68**: 7059–65.
10. Crisswell KA, Krishna G, Zielinski D, *et al.* Use of acridine orange in: flow cytometric evaluation of erythropoietic cytotoxicity. *Mutat Res* 1998; **414**: 49–61.
11. Crisswell KA, Krishna G, Zielinski D, *et al.* Use of acridine orange in: flow cytometric assessment of micronuclei induction. *Mutat Res* 1998; **414**: 63–75.
12. Schmid W. The micronucleus test. *Mutat Res* 1975; **31**: 9–15.
13. Suzuki Y, Nagae Y, Li J, *et al.* The micronucleus test and erythropoiesis: effects of erythropoietin and a mutagen on the ratio of polychromatic to normochromatic erythrocytes (P/N ratio). *Mutagenesis* 1989; **4**: 420–4.
14. Larionov LF. Chemotherapy of malignant tumors. Moscow: Medgiz, 1962. 464 p. (In Russian).
15. Hayashi M, Norppa H, Sofuni T, *et al.* Flow cytometric micronucleus test with mouse peripheral erythrocytes. *Mutagenesis* 1992; **7**: 257–64.
16. Spivak JL. Anemia and erythropoiesis in cancer. *Adv Stud Med* 2002; **2**: 612–9.
17. Spivak JL, Gaskón P, Ludwig H. Anemia management in oncology and hematology. *Oncologist* 2009; **14**: 43–56.
18. Solinas G, Germano G, Mantovani A, *et al.* Tumor-associated macrophages (TAM) as major players of cancer-related inflammation. *J Leukoc Biol* 2009; **86**: 1065–73.
19. Conti I, Rollins BJ. CCL2 (monocyte chemoattractant protein-1) and cancer. *Semin Cancer Biol* 2004; **14**: 149–54.
20. Owen JL, Lopez DM, Grosso JF, *et al.* The expression of CCL2 by T lymphocytes of mammary tumor bearers: Role of tumor-derived factors. *Cell Immunol* 2005; **235**: 122–35.
21. Novakova Z, Hubackova S, Kosar M, *et al.* Cytokine expression and signaling in drug-induced cellular senescence. *Oncogene* 2010; **29**: 273–84.